Atomic Spectroscopy

Article

Ionic Liquid Ferrofluid-Based Preconcentration and Ultra-Trace Determination of As and Se Species in Complex Matrices Using Inductively Coupled Plasma Mass Spectrometry

Yam Nath Gotame and Diane Beauchemin *

Department of Chemistry, Queen's University, 90 Bader Lane, Kingston, ON K7L 3N6, Canada

Received: *March 18, 2024;* ***Revised:*** *May 22, 2024;* ***Accepted:*** *May 23, 2024;* ***Available online:*** *June 14, 2024.*

DOI: 10.46770/AS.2024.042

ABSTRACT: This paper describes the use of an ionic liquid ferrofluid for the preconcentration and simultaneous ultra-trace determination of inorganic As and Se species in waters by inductively coupled plasma mass spectrometry. An ultrasound-assisted sol-gel method was used for the synthesis of silica and titania coated and N-(2-aminoethyl)-3-aminopropyltrimethoxysilane functionalized magnetic nanoparticles (SCTCMNPs-AEAPTMS). The structural features of the SCTCMNPs-AEAPTMS were characterized by Fourier transform infrared spectroscopy, scanning electron microscopy with energy dispersive X-ray spectroscopy, X-ray diffraction, and transmission electron microscopy. Experimental conditions, including the sample solution pH, elution time, and eluent concentration, were optimized. After oxidation of As(III) and Se(IV) to As(V) and Se(VI) by using H_2O_2, the total concentrations of As and Se were determined and those of As(III) and Se(IV) were obtained through subtraction of the concentration of As(V) and Se(VI) from the total concentrations. Under the optimal experimental conditions, the detection limit for As(V) and Se(VI) were 0.3 ng L^{-1} and 0.2 ng L^{-1} respectively. The accuracy of this method was verified by analyzing a certified reference material (1568a Rice Flour): the measured As and Se concentrations agreed with the certified values based on a Student's t-test at the 95% confidence level. The proposed method was also successfully applied to the preconcentration and ultra-trace determination of As and Se species in different water samples.

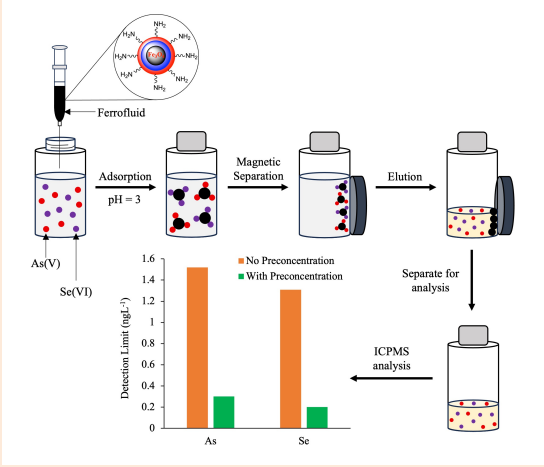

INTRODUCTION

The presence of potentially toxic elements (PTEs) as contaminants in water poses a serious threat to human health, food security, environmental pollution, and global ecosystems.[1] PTEs enter the environment through natural processes (such as volcanic activity, erosion of soil, weathering of minerals, dissolution of minerals, exudates from vegetation, etc.) as well as from anthropogenic sources (such as combustion of fossil fuels, use of pesticides, herbicides and/or preservatives, etc.).[2] Arsenic is a ubiquitous element with serious toxic effects even at low exposure levels when in inorganic form.[3] Consumption of As-contaminated water can lead to various adverse effects, including skin diseases and cardiovascular, genotoxic, mutagenic, and carcinogenic effects.[3] In natural waters, As occurs in both organic and inorganic forms, with inorganic As present in -3, 0, +3, and +5 oxidation states, although -3 and 0 forms are extremely rare species.[3-5] Arsenite (As(III)) has been reported to be several 100 times more toxic than organoarsenic species and 60 times more toxic than arsenate (As(V)).[4,5] In natural waters, As is found as As(III) (*e.g.*, H_3AsO_3, $H_2AsO_3^-$, $HAsO_3^{2-}$) and As(V) (*e.g.*, H_3AsO_4, $H_2AsO_4^-$, $HAsO_4^{3-}$).[6,7] The contamination of natural waters by As is a global issue, prompting the World Health Organization (WHO) and the United States Environmental Protection Agency (US-EPA) to reduce the permissible limits of As in drinking water from 50 to 10

μg L^{-1}.[2] A limit 10 μg L^{-1} was also imposed by the Japanese authorities and European Union for As in drinking water.[8,9]

Selenium is widely recognized as an essential antioxidant for the human body; however, excessive intake can lead to adverse effects.[10] The narrow threshold between essentiality and toxicity, within the range of 50–200 μg d^{-1},[10] emphasizes the importance of regulating Se concentrations in natural waters.[11] The WHO guideline value for Se in drinking water is set at 10 μg L^{-1}.[11] In waters, inorganic Se is primarily found in the forms of selenite (Se(IV), SeO_3^{2-}) and selenate (Se(VI), SeO_4^{2-}). Se(IV) exhibits a higher toxicity than Se(VI).[12-15] Therefore, accurate and selective analytical methods are required for monitoring As and Se species at ultra-trace level in natural water.

Ion chromatography coupled to inductively coupled plasma mass spectrometry (ICPMS) is widely used for the speciation analysis of As and Se.[16] However, because many laboratories cannot afford this combination, a plethora of alternative methods, have been developed, involving cloud point extraction, solid phase microextraction (SPME), *etc.*, in combination with atomic spectrometry detection.[17] Such methods involve separation and preconcentration steps, which are beneficial prior to ICPMS analysis because, in addition to being selective, they can improve the analytical detection limit and sensitivity by orders of magnitude. Solid phase extraction (SPE) is most widely used to this end, primarily due to its simplicity, reusability of the absorbent, minimal consumption of reagent, low cost, and time efficiency, as demonstrated in a recent study involving sequential injection to extract Se(IV) and Se(VI) from water samples onto Dowex 1×8 resin and sequentially elute them prior to measurement by ICPMS.[18]

Magnetic nanoparticles (MNPs) have gained widespread use as sorbents, owing to their stability, high surface area, and easy surface modification.[19] As a lack of analyte selectivity on the surface of sorbent may lead to interference from other species, Fe_3O_4 MNPs should be modified to improve their stability and facilitate functionalization with organic compounds, especially chelating ones that can achieve selective binding of target analytes.[20] TiO_2 is widely used for coating MNPs as it is nontoxic, biologically and chemically inert, environmentally-friendly, resistant to corrosion, and cost-effective. [21-22] However, a TiO_2 coating alone has a high surface area but is thermally unstable and easily loses its surface area.[23] Additionally, although inorganic coatings ensure preservation of the magnetic core from oxidation,[22,24] a TiO_2 coating directly on the Fe_3O_4 core results in undesired interphase interactions that affect the magnetic properties of the MNPs.[24] To overcome these drawbacks, an intermediate SiO_2 layer is required.[25] Overall, a TiO_2 layer with an intermediate SiO_2 layer offers good mechanical properties, porosity, and a thermally stable surface area.[21,22]

In recent years, significant progress has been made in the development and use of liquid magnetic materials, such as ferrofluids, in analytical extractions. [26-28] A ferrofluid is a stable colloidal suspension of coated ferromagnetic nanoparticles in a carrier liquid.[29] Achieving a stable ferrofluid requires a balance between repulsive forces (steric, Brownian motion, and electrostatic forces) and attractive forces (Van der Waals and dipolar attractive forces).[30] Due to the attractive properties of MNPs, they can be readily collected from the sample solutions by using an external magnetic field placed outside the extraction container.[30] Consequently, ferrofluids have found use in diverse fields such as biomedical applications, microelectronics, analytical chemistry, etc.[31] A ferrofluid subjected to a magnetic field for over 35 years remained in a liquid state without any indication of sedimentation, displaying the distinctive pattern of spikes, justifying its stability.[32,33] Hence, a ferrofluid-based preconcentration method should afford stability, reusability, and selectivity.[27,28] Such a method was developed for the selective ultra-trace determination of Pt, Pd, Au and Ag in geological matrices.[34] The ferrofluid used to this end consisted of Fe_3O_4 MNPs with a coating of silica and a second coating of titania, functionalized with 3-mercaptopropyltrimethoxysilane and N-(2-aminoethyl)-3aminopropyltrimethoxysilane, which were suspended in 1-octanol as carrier.

Significant efforts have been directed towards preparing ferrofluids by altering their carrier liquid.[35-37] In this regard, ionic liquids may replace conventional organic carriers due to their unique physiochemical properties.[38] Ionic liquids are considered very stable compounds, having negligible vapour pressure, low flammability, and the ability to remain in a liquid state over a wide range of temperatures.[39] A preconcentration method utilizing a ferrofluid in an ionic liquid carrier focused on the selective ultra-trace determination of carcinogenic Cr(VI) in drinking water.[40] To obtain the ferrofluid, Fe_3O_4 MNPs with a coating of silica were functionalized with L-cysteine and suspended in 1-hexyl-3-methylimidazolium tetrafluoroborate ionic liquid.

The aim of this work was to design an ionic liquid-based ferrofluid for the selective preconcentration and ultra-trace determination of As and Se species in solution by ICPMS. Based on the hard and soft acids and bases theory proposed by R. G. Pearson, soft bases compounds containing N (such as a nitro or amino group) should have a high selectivity towards anionic forms of As(V) and Se(VI), which are typically soft acids. Because interaction between amino modified MNPs and the target analytes should be stronger than with anionic ions that are hard bases (e.g., SO_4^{2-}, NO_3^{2-}, Cl^-, MnO_4^-, etc.),[2] MNPs coated with silica and titania were functionalized with N-(2-aminoethyl)-3-aminopropyltrimethoxysilane (AEAPTMS).[31,33, 35-39] To the best of the authors' knowledge, there is no report on using an ionic liquid-based ferrofluid, where SCTCMNPs-AEAPTMS have two layers of inorganic coatings and are functionalized with organic

compound, for the simultaneous preconcentration of As(V) and Se(VI) in solution and their ultra-trace determination by ICPMS. Flow injection was used for eluate injection to reduce sample handling, the chances of contamination, and memory effects as the entire system is continuously washed with the carrier solution between injections.[41]

EXPERIMENTAL

Standard solutions and certified reference material. Separate 1000 mg L^{-1} As and Se standard stock solutions were made of each species from the following reagents: sodium hydrogen arsenate (98%) and As(III) oxide (99.5%) from Thermo Scientific Chemicals (Waltham, MA, USA), sodium selenate (>95%) (elemental analysis) and sodium selenite from Sigma-Aldrich (St. Louis, MO, USA), and H_2O_2 from J.T. Baker (Phillipsburg, NJ, USA). All As and Se stock solutions were then further diluted to 10 mg L^{-1} prior to being stored at 4 °C in the dark. Multi-elemental standard solutions containing As(V) and Se(VI) anions (0, 0.1, 0.5, 1.0, 1.5, and 3 µg L^{-1}) in 2% (v/v) HNO_3 and used for external calibration were prepared daily from dilution of 10 mg L^{-1} stock solutions in 2% v/v sub-boiled HNO_3 using doubly deionized water (DDW) with 18 MΩ cm resistivity (Arium Pro UV/DI System, Sartorius Stedim Biotech, Goettingen, Germany). A DST-1000 sub-boiling distillation system (Savillex, Minnetonka, MN, USA) was used to purify ACS grade HNO_3 (Fisher Scientific, Ottawa, ON, Canada). Aliquots of 20 mL of standard solutions were preconcentrated using the ferrofluid, followed by elution with 1 mL of 1.6 M HNO_3. Method validation was done using 0.5 g of 1568a Rice Flour from the National Institute of Standards and Technology (Gaithersburg, MD, USA) certified reference material (CRM), which was digested on a hot plate using 25 mL 1 M HNO_3 and 2 mL H_2O_2 for 2 h at 110 °C before dilution to 30 mL with DDW.

Reagents. Acetic acid (ACS reagent grade, glacial), tetraethyl orthosilicate (TEOS), ammonium hydroxide (reagent grade), ethyl alcohol (95% volume), titanium (IV) butoxide ($Ti(OBu)_4$; >97.0%), AEAPTMS (for synthesis), 1-hexyl-3-methylimidazolium tetrafluoroborate (>97%, (HPLC)), and Fe_3O_4 nanoparticles (< 40 nm size, > 98%) were purchased from Sigma-Aldrich (St. Louis, MO, USA). Solution pH was adjusted using either phosphate buffer or sodium acetate/acetic acid buffer. A phosphate buffer solution was prepared by dissolving appropriate amounts of sodium dihydrogen phosphate (NaH_2PO_4), and disodium hydrogen phosphate (Na_2HPO_4), also purchased from Sigma-Aldrich. HCl (reagent grade, 36.5-38%), and HNO_3 (ACS reagent grade, 68-70%) were purchased from Fisher Scientific (Ottawa, ON, Canada). The vessels were cleaned before use by soaking in 10% (v/v) HNO_3 for at least 24 h and then rinsing thoroughly with DDW.

Table 1. ICPMS operating parameters

Parameter	Value
Ar plasma gas flow rate (L min^{-1})	18
Ar auxiliary gas flow rate (L min^{-1})	1.75
Ar sheath gas flow rate (L min^{-1})	0.04
Ar nebulizer gas flow rate (L min^{-1})	0.98
Sampling position (mm)	6.0
RF power (kW)	1.44
CRI H_2 (mL min^{-1})	65
Sample uptake rate (mL min^{-1})	1.0
Monitored analyte (m/z)	^{75}As, ^{78}Se
Dwell time (ms)	10

Instrumentation. All analyses were carried out using a Varian 820MS quadrupole-based ICPMS instrument (Varian Inc., now serviced by Analytik Jena, Jena, Germany) equipped with a collision-reaction interface (CRI), perfluoroalkoxy (PFA) concentric nebulizer, and a Peltier-cooled Scott double-pass spray chamber (SCP Science, Baie d'Urfé, QC, Canada). Manual flow injection was carried out using a Cheminert valve (Valco Instruments Co. Inc., Brockville, ON, Canada) equipped with a 100-µL loop. Additionally, a $Nd_2Fe_{12}B$ magnet was used for separation of SCTCMNPs-AEAPTMS. The instrument operating parameters in Table 1 were used throughout. H_2 was introduced through a hollow CRI skimmer cone to reduce polyatomic interferences. As this did not eliminate the large $^{40}Ar_2^+$ interference on $^{80}Se^+$, $^{78}Se^+$ was monitored instead. Scanning electron microscopy (SEM) and energy dispersive X-ray spectroscopy (EDX) were used to determine the morphology, particle size, surface texture, and elemental composition of SCTCMNPs-AEAPTMS. Measurements were made with a Fei Quanta-250 SEM system coupled with an EDX detector. The sample was placed on carbon tape and put under vacuum in the SEM chamber. Transmission electron microscopy (TEM) was used to characterize the surface morphology and microstructure of SCTCMNPs-AEAPTMS. Measurements were made with a Talos F200i scanning TEM system equipped with Bruker Quanta EDX detector.

Synthesis of SCTCMNPs-AEAPTMS. The synthesis scheme for SCTCMNPs-AEAPTMS is detailed in Fig. S1. Silica coating of MNPs was carried out as in a previous study,[34] using a sol-gel method in basic environment. 4.0 g Fe_3O_4 nanoparticles were dispersed in 200 mL ethanol. The solution was sonicated in a Crest Powersonic Ultrasonic Cleaner under inert N_2 gas for 20 min. Approximately 0.5 mL of TEOS was then added using a precision pipette, followed by the addition of 35 mL of DDW and 40 mL of NH_4OH. The reaction mixture was sonicated for 2 h under N_2 atmosphere. The solution was then poured into a clean beaker. The silica-coated MNPs were separated from solution by placing an external magnet to the bottom of the beaker. The decant was discarded while the silica-coated MNPs were washed with ethanol and DDW at least three times and dried under ambient conditions.

Fig. 1 TEM images of SCTCMNPs-AEAPTMS at (a) 28,500 x and (b) 58,000 x magnification.

Fig. 2 FTIR spectra of the MNPs at different stages of their preparation.

To add a titania coating onto silica-coated MNPs, 2 mL of tetrabutyl orthotitanate was dissolved in 50 mL of ethanol to form a clear solution. Then 4 g silica-coated MNPs were dispersed in the solution and sonicated for 2 h under N_2 atmosphere. The resulting MNPs were magnetically separated, washed with ethanol several times, and dried at room temperature under vacuum. Finally, to graft AEAPTMS, 4 g Fe_3O_4·SiO_2·TiO_2 MNPs were dispersed in 100 mL ethanol and sonicated for 10 min under a N_2 atmosphere. 1 mL AEAPTMS was added to the solution, which was sonicated in an ultrasonic bath at 50 °C for 2 h. The resulting MNPs (SCTCMNPs-AEAPTMS) were washed with water and ethanol at least 3 times and dried at room temperature under vacuum.

Experimental procedure. 80 mg of the resulting SCTCMNPs-AEAPTMS and 200 µL of acetic acid were mixed and heated to 90 °C for 15 min. The acetic acid coated MNPs were dispersed in 100 µL of 1-hexyl-3-methylimidazolium tetrafluoroborate (ionic liquid) and sonicated to obtain a ferrofluid. This ferrofluid was injected into 20 mL of sample solution. The resulting cloudy solution was sonicated for 5 min. SCTCMNPs-AEAPTMS were collected using an external magnet. The supernatant liquid was decanted and collected for ICPMS analysis to determine how much analyte was lost during the separation and check mass balance (Table S1). 1 mL of eluent (1.6 M HNO_3) was added to the collected SCTCMNPs-AEAPTMS, followed by sonication at 50 °C to desorb analytes. The SCTCMNPs-AEAPTMS were again separated using an external magnet, and the eluates were then analyzed by ICPMS. This sorbent allowed the selective determination of As(V) and Se(IV). Determination of the total concentrations of As and Se was performed after addition of H_2O_2 to sample solutions to oxidize As(III) to As(V) and Se(IV) to Se(VI). The concentrations of As(III) and Se(IV) were then obtained through subtraction of the As(V) and Se(VI) concentrations from the total As and Se concentrations respectively.

RESULTS AND DISCUSSION

Different MNPs were tested, including bare Fe_3O_4, Fe_3O_4·SiO_2, Fe_3O_4·SiO_2·TiO_2, Fe_3O_4·SiO_2·MPTMS, Fe_3O_4·SiO_2·L-cysteine, and Fe_3O_4·SiO_2·TiO_2·AEAPTMS. As these MNPs can adsorb anionic species, such as Fe_3O_4·SiO_2·L-cysteine used for the selective preconcentration of anionic Cr(VI),[40] they were tested to see if they could also efficiently retain As(V) and Se(VI) anions. The best analyte recovery was obtained when Fe_3O_4 MNPs were coated with both silica and titania and functionalized with AEAPTMS (Fig. S2).

Characterization of functionalized SCTCMNPs-AEAPTMS. Fig. 1a and b show the average diameter of SCTCMNPs-AEAPTMS, as measured by TEM, to be about 200-250 nm. It also shows that Fe_3O_4 MNPs are surrounded by silica and titania and form a core shell structure with a relatively uniform morphology and homogenous size distribution. The SEM EDX spectra (Fig. S3) indicate the presence of Fe_3O_4 (Fig. S3a), Si after coating with silica (Fig. S3b) and Ti after coating with titania (Fig. S3c). The presence of Fe, Si, Ti, and an excess amount of oxygen are indicated. The determined number of oxygen atom (% atomic) is 48.63%, indicating that the metals existed as oxides. The SEM images (Fig. S4) indicate that Fe_3O_4 MNPs were successfully coated. Because N cannot be detected by EDX, Fourier transform infrared (FTIR) spectroscopy was used to confirm whether the amino compound was successfully grafted onto MNPs. Fig. 2 shows the FTIR spectra for Fe_3O_4, Fe_3O_4·SiO_2, Fe_3O_4·SiO_2·TiO_2, and Fe_3O_4·SiO_2·TiO_2·AEAPTMS. The spectral features of SCTCMNPs-AEAPTMS include the characteristic peak at 2869 cm^{-1} corresponding to an aliphatic C-H bond. The presence of the N–H and -NH_2 bonds in –NH–CH_2–CH_2–NH_2 is indicated by the peaks at 1561 cm^{-1} and 3450 cm^{-1}, respectively. Likewise, the peaks at 1021, 1041, 1091, and 1461 cm^{-1} correspond to Si-O-Fe, Ti-O-H, Si-O-Si, and C-N, respectively. These peaks were absent in the spectrum of bare Fe_3O_4 nanoparticles, indicating that MNPs

Fig. 3 Preconcentration factor (PF) achieved using different concentrations of HNO_3 for elution (analyte from 20 mL sample at pH 3 eluted with 1 mL of eluent (1.6 M HNO_3)); expected PF = 20 [n=3].

Fig. 4 Effect of sample solution pH on adsorption of: a) As species and b) Se species; analyte from 20 mL sample at pH 3 eluted with 1 mL of eluent (1.6 M HNO_3) [n=3].

were coated with silica and titania and functionalized with AEAPTMS. The prepared SCTCMNPS-AEAPTMS were also characterized by X-ray diffraction (XRD) analysis. Fig. S5 shows the XRD patterns of Fe_3O_4 (Fig. S5a), $Fe_3O_4{\cdot}SiO_2$ (Fig. S5b), $Fe_3O_4{\cdot}SiO_2{\cdot}TiO_2$ (Fig. S5c), and $Fe_3O_4{\cdot}SiO_2{\cdot}TiO_2{\cdot}$AEAPTMS (Fig. S5d). In Fig. S5a, the diffraction peaks at 16°, 35°, 39°, and 65° are characteristic of Fe_3O_4. The consistent XRD patterns after different steps (Fig. S5) indicate that the structure of the Fe_3O_4 MNPs does not change during the entire process. The SiO_2 and TiO_2 layers were deposited on the MNPs using the sol-gel method, producing an amorphous TiO_2 coating, which would require calcination at elevated temperatures to be converted to crystalline form (anatase or rutile).[42-43] As, before XRD analysis, the SCTCMNPs were simply dried at room temperature in a vacuum, this could explain why the characteristic peaks of TiO_2 are not visible in Fig. S5.

Selection of eluent concentration and eluent volume. The adsorption of Se(VI) and As (V) decreased when the pH of sample solution was below 1.5 (not shown), indicating that the retained As(V) and Se(VI) can be desorbed with high acidity solution. Among the strong acids (HCl, HNO_3, H_2SO_4), HNO_3 was selected because it induces fewer interference during ICPMS measurements. The effect of HNO_3 concentration in the range of 0.1-2 mol L^{-1} on elution of adsorbed As(V) and Se(VI) is summarized in Fig. 3. The recoveries were highest when using at least 1.6 M HNO_3. However, because more than 2 M HNO_3 may cause the loss of functionality of the adsorbent, 1.6 M HNO_3 was selected as eluent for subsequent experiments. The effect of eluent volume (from 1 to 5 mL) was also studied while keeping the concentration of HNO_3 at 1.6 M (Table S2). Because 1.6 M HNO_3 was sufficient to quantitatively recover As(V) and Se(VI), it was used for subsequent experiments.

Effect of sample solution pH on adsorption. The effect of pH on retention of As(V) and Se(VI) by amino-modified MNPs was investigated in the pH range of 1-6, which was adjusted by using a phosphate buffer solution while keeping all other parameters constant. Fig. 4 shows that good recoveries resulted when the pH was 3.0, which was selected for subsequent experiments. The sorption of metal ions usually depends on the surface charge of nanoadsorbent due to protonation and deprotonation of chelating materials as well as on the metal ion species present in solution.[44]

In an acidic medium, the surface of functionalized MNPs would be positively charged from abundant protonated amino groups (-NH_3^+), resulting in high adsorption efficiency of As(V) and Se(VI), specifically AsO_4^{3-} and SeO_4^{2-}. Adsorption of anionic As(V) or Se(VI) likely occurs through electrostatic attractions with the protonated amine groups in low pH conditions, as illustrated in Fig. S6. Additionally, as the point of zero charge value of TiO_2 is 6.25,[45] maintaining the pH below 6.5 could result in a positive surface charge of titania and lead to it adsorbing anionic species of As and Se. In contrast, because As(III) and Se(IV) mostly exist as neutral species (*i.e.*, H_3AsO_3 and H_2SeO_3), they are hardly adsorbed by the MNPs. At alkaline pH values, protonation of the amino group would weaken and the charge of adsorbent would become negative, resulting in poor adsorption of As(V) and Se(VI). [46-48]

According to Hosseini & Nazemi, As(III) and Se(IV) could be oxidized to As(V) and Se(VI) by 10% H_2O_2 dissolved in 0.2 M HCl at room temperature.[49] In this work, 4 mL of 10% H_2O_2

Fig. 5 Effect of adsorption and elution times on As(V) and Se(VI) recovery (analyte from 20 mL sample at pH 3 eluted with 1 mL of eluent (1.6 M HNO_3)) [n=3].

Table 2. Tolerance concentrations of co-existing ions

Ions	Tolerance limit of As(V) and Se (VI) (mg L^{-1})
Na^+	400
K^+	500
Ca^{2+}	200
Mg^{2+}	300
Ba^{2+}	300
Fe^{2+}, Fe^{3+}	200
Cu^{2+}	500
Al^{3+}	200
Ti^{4+}	50
Pd^{4+}, Pt^{2+}	25
Ag^+, Au^{3+}	20
PO_4^{2-}	50
Cl^-	1000
SO_4^{2-}	1500
NO_3^-	2000

dissolved in 0.2 M HCl was sufficient to quantitatively transform As(III) and Se(IV) in 20-mL solutions to As(V) and Se(VI), respectively (Fig. S7). The solution was then shaken for 5 min before being boiled to remove residual H_2O_2.

Effect of adsorption and elution times. To minimize the time required for sample processing, the effect of ultrasonication time on analyte adsorption and elution was studied with the optimized amount of sorbent (80 mg) (Fig. S8). Fig. 5 indicates that more than 90% adsorption and elution occurred in 4 min and 5 min respectively. Therefore, 4 min for adsorption and 5 min for elution were used in subsequent experiments.

Influence of sample volume. To obtain a high preconcentration factor, a large volume of sample solution and small volume of eluent are required. The effect of sample volume was studied using 10, 20, 60, 100, 150, and 200 mL of solution containing 0.4 µg L^{-1} As and Se. Recoveries are almost quantitative up to 150 mL, however, the extraction efficiency slightly decreased when the sample volumes were larger than this volume. Hence, 150 mL of sample solution was selected as the largest sample volume for the preconcentration of analytes. The best analyte recovery was achieved with 20 mL of sample solution and was used in the subsequent experiments.

Effect of coexisting ions. The effect of potential interfering ions on the preconcentration/separation and determination of As(V) and Se(VI) was investigated using the optimal method described above. Known amounts of anions and cations were individually added to 20 mL of solution containing 0.4 µg L^{-1} As(V) and Se(VI), preconcentrated using a ferrofluid containing SCTCMNPs-AEAPTMS, followed by elution with 1 mL of 1.6 M HNO_3. The tolerance limit of coexisting ions is summarized in Table 2. This indicates that amino functionalised silica and titania coated MNPs show good selectivity for As(V) and Se(VI) and should thus be suitable for the analysis of environmental water samples.

Detection limits. Standard solutions of As(V) and Se(VI) containing (0, 0.1, 0.5, 1.0, 1.5 and 3.0 µg L^{-1}) in HNO_3 were used for external calibration. 20 mL of solutions were preconcentrated using ferrofluid and eluted with 1 mL of 1.6 M HNO_3. Good correlation (R^2 > 0.9961) was obtained for all analytes. The detection limits for As(V) and Se(VI), calculated as 3 *s*/m (where *s* is the standard deviation of 10 measurements of method blank and m is the slope of the calibration curve) and which are 2 ng L^{-1} and 1 ng L^{-1} without preconcentration, respectively, improved to 0.3 ng L^{-1} and 0.2 ng L^{-1}, respectively. The less than 20-fold improvement in detection limit is likely a result of blank contamination, as there is no clean room facility on campus for sample preparation. Despite this limitation that was out of the authors' control, these detection limits are generally lower than those reported previously as shown in Table S3. The detection limit for As(V) is similar to that previously obtained by solvent bar microextraction–electrothermal vaporization (ETV) ICPMS[52] without requiring the acquisition of an expensive ETV system. The method involving flow injection capillary microextraction on ordered mesoporous Al_2O_3 with ICPMS detection, which provides 0.7 ng L^{-1} detection limit for As(V) after only a 5-fold preconcentration, ties up the ICPMS instrument for the whole preconcentration step, limiting the sampling frequency to 8 samples h^{-1}. Its sample uptake rate is indeed limited to 0.1 mL min^{-1} because a capillary having its inner surface coated with Al_2O_3 is used with a peristaltic pump. In contrast, the proposed batch approach can be applied to many samples in parallel, the ICPMS instrument only being used to analyze the leachates, in turn enabling a much higher sampling frequency of at least 60 samples h^{-1}.

Accuracy, sorbent regeneration and sample analysis. To validate the proposed method, 50 µL of 1568a Rice Flour digest in 1 M HNO_3 medium was diluted to 20 mL using DDW and adjusted to pH 3.00 using phosphate buffer solution. Following application of the proposed preconcentration method, the eluate was analyzed via ICPMS using matrix-matched external calibration. As can be seen in Table S4, the measured total

Table 3. Determination of arsenic and selenium species in spiked water samples (analyte from 20 mL sample at pH 3 eluted with 1 mL of eluent (1.6 M HNO_3)); ± standard deviation, µg L^{-1} [n=3]

Sample	Spiked (µg L^{-1})		Measured (µg L^{-1})				Recovery (%)		
	As(III)	As(V)	As(V)		As(III)	As(V)	As(V)		As(III)
Tap water	-	-	Not detected	Tap water	-	-	Not detected	Tap water	-
	0.31	0.45	0.43 ± 0.03		0.31	0.45	0.43 ± 0.03		0.31
Mineral water	-	-	Not detected	Mineral water	-	-	Not detected	Mineral water	-
	0.31	0.45	0.44 ± 0.02		0.31	0.45	0.44 ± 0.02		0.31
	Se(IV)	**Se(VI)**	**Se(VI)**		**Se(IV)**	**Se(VI)**	**Se(VI)**		**Se(IV)**
Tap water	-	-	Not detected	Tap water	-	-	Not detected	Tap water	-
	0.31	0.45	0.43 ± 0.05		0.31	0.45	0.43 ± 0.05		0.31
Mineral water	-	-	Not detected	Mineral water	-	-	Not detected	Mineral water	-
	0.31	0.45	0.42 ± 0.04		0.31	0.45	0.42 ± 0.04		0.31

concentrations are in agreement with the certified values based on a Student's t-test at the 95% confidence level. The SCTCMNPs-AEAPTMS can be reused up to five times without significant loss of analytical performance (Fig. S9). This is acceptable, considering that 4 g of SCTCMNPs-AEAPTMS could be prepared in one batch and only 80 mg of SCTCMNPs-AEAPTMS was used per extraction. Application of the method to real samples yielded the results in Table 3 for As and Se species. As neither Kingston tap water nor the mineral water bought at a local grocery store contained detectable levels of As and Se, they were spiked with As(III), As(V), Se(IV) and Se(VI). Good recoveries of As and Se species were obtained, in the range of 90-98%.

CONCLUSION

In brief, silica and titania coated and N-(2-aminoethyl)-3-aminopropyltrimethoxysilane functionalized MNPs were successfully synthesized and applied to the simultaneous determination of As(V) and Se(VI) in anionic form in aqueous solution by ICPMS. The sorbent adsorbed analytes within 4 min with high selectivity, and elution took 5 min. This translated in high accuracy and sensitivity, thereby allowing the enrichment and determination of ultra-trace metal ion species in real samples. The reusability of the sorbent was greater than 5 cycles without any loss in sorption efficiency. The detection limits of analytes are better than those of previous SPE methods in the literature (Table S3). Moreover, it was successfully applied to a rice flour CRM and provided accurate results for As and Se. Despite the unique characteristics of ionic liquids, they suffer from some limitations, including high cost, low biodegradability, and complicated synthesis process, which could be overcome by replacing ionic liquids with supramolecular solvents and deep eutectic solvents. Future work will aim to characterize the magnetic ionic liquid using vibrating sample magnetometry. In addition, the approach will be extended to the separation/preconcentration of other PTEs in anionic form in water.

ASSOCIATED CONTENT

Supporting information (Figs. S1-S9 and Table S1-S4) is available at www.at-spectrosc.com/as/home

AUTHOR INFORMATION

Diane Beauchemin received her Ph.D. in 1984 from Université de Montréal. She is a professor (Full) at Queen's University. Her research efforts are focused on inductively coupled plasma mass spectrometry (ICPMS) and ICP optical emission spectrometry (OES) from both fundamental and application perspectives, and expanding the range of application of ICPMS/OES to geochemical exploration, risk assessment of food safety, characterization of nanoparticles, and forensic analysis. She has been working as member of editorial board for *Atomic Spectroscopy*. Diane Beauchemin won the Alan Date Memorial Award (1988) from VG Elemental, the Distinguished Service Award (2001) from Spectroscopy Society of Canada, the Maxxam Award (2017) and Clara Benson Award (2019) from Canadian Society for Chemistry, the Gerhard Herzberg Award (2018) from the Canadian Society for Analytical Sciences and Spectroscopy, and, and the Environment Division Research and Development Dima Award from the Chemical Institute of Canada. She is author or co-author of over 180 articles published in peer-reviewed scientific journals.

Corresponding Author

*D. Beauchemin

Email address: diane.beauchemin@queensu.ca

Notes

The authors declare no competing financial interest.

ACKNOWLEDGMENTS

We gratefully acknowledge the Natural Sciences and Engineering Council of Canada (CRDPJ 503887-16) as well as Activation

Laboratories Ltd. for financial support. YNG also thanks Queen's University School of Graduate Studies for a graduate award.

REFERENCES

1. O. Akpor and M. Muchie, *Int. J. Phys. Sci.*, 2010, **5**, 1807–1817. https://academicjournals.org/journal/IJPS/article-abstract/00E529A31916
2. H. Peng, N. Zhang, M. He, B. Chen, and B. Hu, *Talanta*, 2015, **131**, 266–272. https://doi.org/10.1016/j.talanta.2014.07.054
3. D. Q. Hung, O. Nekrassova, and R. G. Compton, *Talanta*, 2004, **64**, 269–277. https://doi.org/10.1016/j.talanta.2004.01.027
4. H. G. Seiler, A. Sigel, and H. Sigel, in Handbook on Metals in Clinical and Analytical Chemistry, Marcell Dekker Inc. New York, 1994. https://worldcat.org/title/29184449
5. M. A. Karimi, A. Mohadesi, A. Hatefi-Mehrjardi, S. Z. Mohammadi, J. Yarahmadi, and A. Khayrkhah, *J. Chem.*, 2014, **2014**, 248065. https://doi.org/10.1155/2014/248065
6. I. Ali, T. A. Khan, and M. Asim, *Sep. Purif. Rev.*, 2011, **40**, 25–42. https://doi.org/10.1080/15422119.2011.542738
7. U. Beker, L. Cumbal, D. Duranoglu, I. Kucuk, and A. K. Sengupta, *Environ. Geochem. Health*, 2010, **32**, 291–296. https://doi.org/10.1007/s10653-010-9301-2
8. C. I. S. Narcise, L. dlC. Coo, and F. R. del Mundo, *Talanta*, 2005, **68**, 298–304. https://doi.org/10.1016/j.talanta.2005.08.055
9. P. L. Smedley, and D. G. Kinniburgh, *Appl. Geochem.*, 2002, **17**, 517–568. https://doi.org/10.1016/S0883-2927(02)00018-5
10. F. Xu, J. Hu, J. Zhang, X. Hou, and X. Jiang, *Appl. Spectrosc. Rev.*, 2018, **53**, 333–348. https://doi.org/10.1080/05704928.2017.1323310
11. K. L. LeBlanc, P. Kumkrong, P. H. J. Mercier, and Z. Mester, *Sci. Total Environ.*, 2018, **640–641**, 1635–1651. https://doi.org/10.1016/j.scitotenv.2018.05.394
12. M. P. Rayman, H. G. Infante, and M. Sargent, *Br. J. Nutr.*, 2008, **100**, 238–253. https://doi.org/10.1017/S0007114508922522
13. K. Šindelářová, J. Záková, J; Tremlová, O. Mestek, L. Praus, A. Kaňa, J. Najmanová, and P. Tlustoš, *Food Addit. Contam. A.*, 2015, **32**, 2027–2038. https://doi.org/10.1080/19440049.2015.1099744
14. X. Wang, L. Wu, J. Cao, X. Hong, R. Ye, W. Chen, and T. Yuan, *Food Addit. Contam. A*, 2016, **33**, 1190–1199. https://doi.org/10.1080/19440049.2016.1189807
15. A. K. Das, M. de la Guardia, and M. L. Cervera, *Talanta*, 2001, **55**, 1–28. https://doi.org/10.1016/S0039-9140(01)00400-3
16. S. M. Rangan, R. Krajmalnik-Brown, and A. G. Delgado, *Environ. Eng. Sci.*, 2021, **38**, 626–634. https://doi.org/10.1089/ees.2020.0347
17. X. Yu, C. Liu, Y. Guo, and T. Deng, *Molecules*, 2019, **24**, 926. https://doi.org/10.3390/molecules24050926
18. J. Yang, Y. Chen, K. Shi, K. Hu, R. Li, X. Gao, Q. Wang, W. Zhang, Y. Zhu, Y. Wang, J. He, T. Liu, and X. Hou, *Chin. Chem. Lett.*, 2022, **33**, 3444–3450. https://doi.org/10.1016/j.cclet.2022.03.002
19. H. Xu, N. Tong, L. Cui, Y. Lu, and H. Gu, *J. Magn. Magn. Mater.*, 2007, **311**, 125–130. https://doi.org/10.1016/j.jmmm.2006.11.173
20. L. Zhang, Y. Zhai, X. Chang, Q. He, X. Huang, and Z. Hu, *Microchim. Acta*, 2009, **165**, 319–327. https://doi.org/10.1007/s00604-009-0137-3
21. S. Dagher, A. Soliman, A. Ziout, N. Tit, A. Hilal-Alnaqbi, S. Khashan, F. Alnaimat, and J. A. Qudeiri, *Mater. Res. Express*, 2018, **5**, 65518. https://doi.org/10.1088/2053-1591/aacad4
22. L. De Matteis, R. Fernández-Pacheco, L. Custardoy, M. L. García-Martín, J. M. de la Fuente, C. Marquina, and M. R. Ibarra, *Langmuir*, 2014, **30**, 5238–5247. https://doi.org/10.1021/la500423e
23. R. Y. Hong, J. H. Li, S. Z. Zhang, H. Z. Li, Y. Zheng, J. Ding, and D. G. Wei, *Appl. Surf. Sci.*, 2009, **255**, 3485–3492. https://doi.org/10.1016/j.apsusc.2008.09.071
24. R. Ghosh Chaudhuri, and S. Paria, *Chem. Rev.*, 2012, **112**, 2373–2433. https://doi.org/10.1021/cr100449n
25. S. Watson, J. Scott, D. Beydoun, and R. Amal, *J. Nanopart. Res.*, 2005, **7**, 691–705. https://doi.org/10.1007/s11051-005-7520-8
26. M. Sajid, K. Kalinowska, and J. Płotka-Wasylka, *J. Mol. Liq.*, 2021, **339**, 116901. https://doi.org/10.1016/j.molliq.2021.116901
27. M. Sajid, *Trac-Trends Anal. Chem.*, 2019, **113**, 210–223. https://doi.org/10.1016/j.trac.2019.02.007
28. K. D. Clark, O. Nacham, J. A. Purslow, S. A. Pierson, and J. L. Anderson, *Anal. Chim. Acta*, 2016, **934**, 9–21. https://doi.org/10.1016/j.aca.2016.06.011
29. G. Piying, F. Ruolan, Z. Huaizhu, and L. Zhiqiang, *Anal. Lett.*, 1998, **31**, 1095–1106. https://doi.org/10.1080/00032719808002845
30. M. D. Farahani, F. Shemirani, and M. Gharehbaghi, *Talanta*, 2013, **109**, 121–127. https://doi.org/10.1016/j.talanta.2013.01.061
31. N. Fasih Ramandi, and F. Shemirani, *Talanta*, 2015, **131**, 404–411. https://doi.org/10.1016/j.talanta.2014.08.008
32. O. Oehlsen, S. I. Cervantes-Ramírez, P. Cervantes-Avilés, and I. A. Medina-Velo, *ACS Omega*, 2022, **7**, 3134–3150. https://doi.org/10.1021/acsomega.1c05631
33. H. Wang, C. Bi, Y. Zhang, L. Zhang, and F. Zhou, *Sci. Rep.*, 2021, **11**, 8887. https://doi.org/10.1038/s41598-021-88407-0
34. Y. N. Gotame, V. Gandolfi, and D. Beauchemin, *Atom. Spectrosc.*, 2022, **43**, 443–449. https://doi.org/10.46770/AS.2022.229
35. M. Gharehbaghi, M. D. Farahani, and F. Shemirani, *Anal. Methods*, 2014, **6**, 9258–9266. https://doi.org/10.1039/C4AY01531B
36. C. Guerrero-Sanchez, T. Lara-Ceniceros, E. Jimenez-Regalado, M. Raşa, and U. S. Schubert, *Adv. Mater.*, 2007, **19**, 1740–1747. https://doi.org/10.1002/adma.200700302
37. F. C. C. Oliveira, L. M. Rossi, R. F. Jardim, and J. C. Rubim, *J. Phys. Chem. C*, 2009, **113**, 8566–8572. https://doi.org/10.1021/jp810501m
38. H. Ohno, in Electrodeposition from Ionic Liquids, ed. F. Endres, D. MacFarlane, and A. Abbott, Wiley-VCH Verlag GmbH & Co. KGaA, 2008, pp. 47–82. https://doi.org/10.1002/9783527622917
39. E. Altin, J. Gradl, and W. Peukert, *Chem. Eng. Technol.*, 2006, **29**, 1347–1354. https://doi.org/10.1002/ceat.200600135
40. Y. N. Gotame, and D. Beauchemin, *Atom. Spectrosc.*, 2024, **45**, 115–122. https://www.at-spectrosc.com/as/article/pdf/2024019
41. Y. Madrid, M. Wu, Q. Jin, and G. M. Hieftje, *Anal. Chim. Acta*, 1993, **277**, 1–8. https://doi.org/10.1016/0003-2670(93)85083-V
42. R. E. Kalan, S. Yaparatne, A. Amirbahman, and C. P. Tripp, *Appl. Catal. B-Environ.*, 2016, **187**, 249–258. https://doi.org/10.1016/j.apcatb.2016.01.008

43. H. Niu, Q. Wang, H. Liang, M. Chen, C. Mao, J. Song, S. Zhang, Y. Gao, and C. Chen, *Materials*, 2014, **7**, 4034–4044. https://doi.org/10.3390/ma7054034
44. H. Ahmad, A. Ahmad, and S. S. Islam, *Microchim. Acta*, 2017, **184**, 2007–2014. https://doi.org/10.1007/s00604-017-2214-3
45. H. Rashidi Nodeh, W. A. Wan Ibrahim, I. Ali, and M. M. Sanagi, *Environ. Sci. Pollut. Res.*, 2016, **23**, 9759–9773. https://doi.org/10.1007/s11356-016-6137-z
46. C. Xiong, M. He, and B. Hu, *Talanta*, 2008, **76**, 772–779. https://doi.org/10.1016/j.talanta.2008.04.031
47. D. Chen, C. Huang, M. He, and B. Hu, *J. Hazard. Mater.*, 2009, **164**, 1146–1151. https://doi.org/10.1016/j.jhazmat.2008.09.022
48. A. Afkhami, T. Madrakian, and A. A. Assl, *Talanta*, 2001, **55**, 55–60. https://doi.org/10.1016/S0039-9140(01)00391-5
49. M. S. Hosseini and S. Nazemi, *Analyst*, 2013, **138**, 5769–5776. https://doi.org/10.1039/C3AN00869J
50. W. Hu, F. Zheng, and B. Hu, *J. Hazard. Mater.*, 2008, **151**, 58–64. https://doi.org/10.1016/j.jhazmat.2007.05.044
51. F. Shemirani, M. Baghdadi, and M. Ramezani, *Talanta*, 2005, **65**, 882–887. https://doi.org/10.1016/j.talanta.2004.08.009
52. X. Pu, B. Chen, and B. Hu, *Spectroc. Acta B*, 2009, **64**, 679–684. https://doi.org/10.1016/j.sab.2009.06.001
53. I. López-García, R. E. Rivas, and M. Hernández-Córdoba, *Talanta*, 2011, **86**, 52–57. https://doi.org/10.1016/j.talanta.2011.07.105
54. J.-R. Chen, W.-H. Tsai, and C.-K. Su, *Anal. Chim. Acta*, 2023, **1271**, 341489. https://doi.org/10.1016/j.aca.2023.341489
55. C.K. Su, and W.C. Chen, *Microchim. Acta*, 2018, **185**, 268. https://doi.org/10.1007/s00604-018-2812-8
56. Z. Chen, B. Chen, M. He, and B. Hu, *Microchim. Acta*, 2020, **187**, 48. https://doi.org/10.1007/s00604-019-4055-8
57. L.Y. Zhao, Q.Y. Zhu, L. Mao, Y.J. Chen, H.Z. Lian, and X. Hu, *Talanta*, 2019, **192**, 339–346. https://doi.org/10.1016/j.talanta.2018.09.064
58. F. Zheng and B. Hu, *J. Anal. At. Spectrom.*, 2009, **24**, 1051–1061. https://doi.org/10.1039/B900057G
59. S. Li and N. Deng, *Anal. Bioanal. Chem.*, 2002, **374**, 1341–1345. https://doi.org/10.1007/s00216-002-1591-5
60. Y. Wang, J. Xie, Y. Wu, X. Hu, C. Yang, and Q. Xu, *Talanta*, 2013, **112**, 123–128. https://doi.org/10.1016/j.talanta.2013.03.014
61. C.Z. Huang, B. Hu, M. He, and J.K. Duan, *J. Mass Spectrom.*, 2008, **43**, 336–345. https://doi.org/10.1002/jms.1321